Chemosphere 234 (2019) 450–460

Contents lists available at ScienceDirect

Chemosphere

journal homepage: www.elsevier.com/locate/chemosphere

# Sulfide drives hydroxyl radicals production in oxic ferric oxyhydroxides environments

Elias Niyuhire, Songhu Yuan*, Wenjuan Liao, Jian Zhu, Xixiang Liu, Wenjing Xie, Ao Qian

*State Key Laboratory of Biogeology and Environmental Geology, China University of Geosciences, 388 Lumo Road, Wuhan, 430074, PR China*

## HIGHLIGHTS

- ·OH can be produced in oxic Fe(III)-bearing environments perturbed by sulfide.
- Surface-bound Fe(II) and Fe(II) in the solid phase or FeS were produced in sulfide/Fe(III)/$O_2$ systems.
- $O_2$ activation by surface-bound Fe(II) and/or Fe(II) in the solid phase or FeS was responsible for ·OH production.
- The produced ·OH could oxidize organic contaminants.
- A new abiotic pathway was proposed for dark ·OH production in the environment.

## GRAPHICAL ABSTRACT

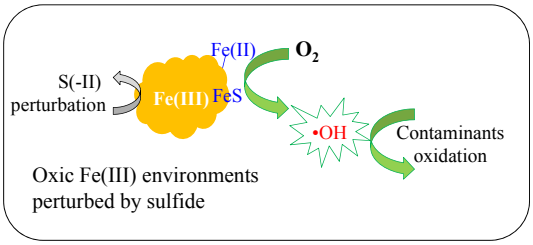


A new abiotic pathway of dark ·OH production

## ARTICLE INFO

*Article history:*
Received 13 January 2019
Received in revised form
15 May 2019
Accepted 5 June 2019
Available online 15 June 2019

Handling Editor: Dr Patryk Oleszczuk

*Keywords:*
Iron oxyhydroxides
Sulfide
Hydroxyl radicals
Contaminant transformation
Redox-dynamic

## ABSTRACT

Perturbation of Fe(III)-bearing oxic environments by reduced species such as sulfide occurs widely in natural and engineered systems. However, whether hydroxyl radicals (·OH) can be produced in these environments remains unexplored. Here we show that sulfide drives ·OH production in Fe(III) oxyhydroxides suspensions under neutral and oxic conditions. For lepidocrocite, ferrihydrite and goethite suspensions at 11.2 mM Fe, the addition of 0.5 mM sulfide produced 14.2, 14.3 and 22.4 μM ·OH within 120 min, respectively. With addition of sulfide to lepidocrocite suspensions at 11.2 mM Fe, the cumulative ·OH concentration within 120 min increased from 0 to 14.2, 25.2, 52.6 and 63.1 μM when sulfide dosage increased from 0 to 0.5, 2.5, 5 and 7.5 mM, respectively. At a fixed sulfide dosage of 5 mM, the cumulative ·OH concentration increased with increasing the number of sulfide additions. The mechanisms of ·OH production were attributed to the generation of surface-bound Fe(II), most likely in the form of $>Fe^{II}OH_2^+$, and Fe(II) in the solid phase or FeS from the reactions between sulfide and Fe(III), followed by $O_2$ activation. ·OH production could take place until depletion of sulfide. Finally, we found that the generated ·OH could oxidize the coexisting redox-active substances like phenol under neutral and oxic conditions. Our findings reveal that sulfide perturbation of Fe(III)-bearing oxic environments is a new source of ·OH, and contaminants oxidation by ·OH necessitates consideration in these environments.



## 1. Introduction

Hydroxyl radicals (·OH), strongly reactive oxidants, play a crucial role in the transformation of contaminants in aqueous environments. Due to their environmental significance, many studies have been devoted to identifying the sources of ·OH production (Page et al., 2013; Tong et al., 2016; Trusiak et al., 2018; Vione et al., 2006). ·OH production in the environment has been early attributed to photolytic processes (Manning et al., 2005; Mopper and

* Corresponding author.
*E-mail address:* yuansonghu622@cug.edu.cn (S. Yuan).

https://doi.org/10.1016/j.chemosphere.2019.06.037
0045-6535/

Zhou, 1990). In the recent decade, it was discovered that •OH could be produced by biotic and abiotic processes in dark environments. For example, •OH can be produced by a wide range of fungi through enzymatic mediated extracellular redox cycling of quinones and iron (Gómez-Toribio et al., 2009; Moyo et al., 2017), and it can also be produced abiotically in redox-dynamic environments (Minella et al., 2015; Page et al., 2012, 2013; Tong et al., 2016). The abiotic •OH production in the dark is attributed to the interaction of molecular oxygen ($O_2$) with reduced species such as natural organic matter (NOM) and ferrous iron (Fe(II)) (Minella et al., 2015; Page et al., 2012, 2013; Tong et al., 2016). Most reduced species can activate $O_2$ to generate reactive oxygen species (ROS) such as superoxide ($O_2^{\bullet-}$) and hydrogen peroxide ($H_2O_2$) (Cheng et al., 2016; Murphy et al., 2014, 2016; Yuan et al., 2017), but specific Fe(II) species are required for converting $H_2O_2$ to •OH (Tong et al., 2016; Trusiak et al., 2018).

There are two types of redox perturbations which may be regarded to be responsible for abiotic •OH production in the dark. One is the perturbation of anoxic environments by $O_2$. Many investigations documented that oxygenation of anoxic waters and sediments produced •OH (Page et al., 2012, 2013; Tong et al., 2016; Trusiak et al., 2018). The other one is the perturbation of oxic environments by reduced species discharged or diffused from anoxic environments. However, whether •OH can be produced by this type of redox perturbation remains unexplored. Perturbation of oxic environments by reduced species is very common in both natural (Brüchert et al., 2003; Eggleton and Thomas, 2004; Ohde and Dadou, 2018) and engineered systems (Reynolds and Barrett, 2003). Sulfide is an important reduced species occurring naturally in anoxic environments and used widely in the chemical industry (Reverberi et al., 2016). In natural environments, sulfide-bearing waters such as groundwater can diffuse or discharge into oxic environments like shallow aquifers and soils/sediments (Jayalath et al., 2016; Payne and Stolt, 2017; Tostevin et al., 2016), and large amounts of sulfide can be discharged in hot springs (Giampaoli et al., 2013). For example, sulfide up to 22 mM was measured in sediment pore waters (Fenchel, 1969; Brüchert et al., 2003), at 400 μM was quantified in a surface water due to storm vents (Luther et al., 2004), and up to 1 mM was measured in hot springs (Giampaoli et al., 2013; Fazlzadeh et al., 2018). In engineered systems, sulfide-containing wastes and wastewaters may leak or discharge into the oxic surface environments (Held et al., 2006; Reynolds and Barrett, 2003). Fe(III) is abundant in oxic soils and sediments. Fe (III) oxyhydroxides account for approximately 40%–45% of the total iron in sediments supplied to the ocean (Poulton and Raiswell, 2002). Upon redox perturbation of oxic environments by reduced species, one has coexistence of sulfide, $O_2$ and Fe(III). Nevertheless, the ternary mixture is thermodynamically unstable. Sulfide tends to reduce Fe(III) to Fe(II) (Eq. (1)), and subsequently Fe(II) reacts with $O_2$ to generate ROS following the Haber-Weiss mechanism (Eqs. (2)–(4) (King et al., 1995; Rose and Waite, 2002). As $O_2$ is in excess under oxic conditions, the redox reactions are expected to occur until depletion of sulfide.

$$S(\text{-II}) + Fe(III) \rightarrow S_0 + Fe(II) \quad (1)$$

$$Fe(II) + O_2 \rightarrow Fe(III) + O_2^{\bullet-} \quad (2)$$

$$Fe(II) + O_2^{\bullet-} + 2H^+ \rightarrow Fe(III) + H_2O_2 \quad (3)$$

$$Fe(II) + H_2O_2 \rightarrow Fe(III) + {}^{\bullet}OH + OH^- \quad (4)$$

Here we hypothesize that perturbation of oxic ferric oxyhydroxides by sulfide could produce •OH. Virtually, production of $O_2^{\bullet-}$ and $H_2O_2$, the precursors of •OH, has been documented in recent years. Murphy et al. added sulfide into real sediment suspensions under oxic conditions and measured the generation of $O_2^{\bullet-}$ and $H_2O_2$ (Murphy et al., 2014, 2016). Hydrous ferric oxides (HFO or ferrihydrite) were identified as the predominant Fe(III) oxyhydroxides for sulfide oxidation, and the generated aqueous Fe(II) was involved in $O_2$ activation to generate $O_2^{\bullet-}$ and $H_2O_2$ (Murphy et al., 2014, 2016). However, it remains elusive whether •OH can be produced in the system because $H_2O_2$ decomposition to •OH (Eq. (4)) depends greatly on Fe(II) speciation. The aqueous $Fe^{2+}$ cannot effectively decompose $H_2O_2$ to •OH under circumneutral pH (Keenan and Sedlak, 2008a; Zhang and Yuan, 2017). It is also not clear whether other Fe(III) oxyhydroxides with a higher degree of crystallinity than HFO can function similarly for ROS production in sulfide/Fe(III)/$O_2$ systems.

Therefore, the goals of this study are (1) to ascertain whether •OH can be produced when Fe(III) oxyhydroxides-bearing oxic environments are perturbed by sulfide, (2) to identify the specific Fe(II) species contributing to •OH production in sulfide/Fe(III)/$O_2$ environments, and (3) to evaluate the environmental significance of •OH for substance transformation. To reach these goals, we first measured •OH production upon addition of sulfide to three types of common Fe(III) oxyhydroxides under oxic conditions. Then, we further measured •OH production and Fe(II) and sulfide variations with single and multiple sulfide additions. The Fe(II) species contributing to •OH production were explored by the addition of 2,2′-bipyridine (BPY) and Raman and X-ray photoelectron spectroscopy (XPS). The environmental significance was examined by the oxidation of phenol, which was used as a model contaminant because phenolic compounds are widely found in the environment (Lin et al., 2016; Wang and Kannan, 2018; Lu et al., 2019) and the reaction of phenol with •OH has been studied extensively (Pera-Titus et al., 2004).

## 2. Materials and methods

### 2.1. Chemicals

Sodium benzoate (BA, 99.5%), 4-Hydroxybenzoic acid (*p*-HBA, 99%), 2,2′-bipyridine (BPY, 99.5%) and ferrous chloride tetrahydrate ($FeCl_2 \cdot 4H_2O$, 99%) were purchased from Sinopharm Chemical Reagent Co., Ltd., China. Sodium sulfide nonahydrate ($Na_2S \cdot 9H_2O$, 98.0%) was purchased from Shanghai Tongya Chemical Technology Co., Ltd. Deionized (DI) water (18.2 MΩ cm) from a Heal Force NW ultrapure water system was used in all the experiments. The presence of ROS (•OH, $O_2^{\bullet-}$ and $H_2O_2$) in the DI water has been proven to be negligible in our previous study (Zhang and Yuan, 2017). All the other chemicals were of analytical grade.

### 2.2. Synthesis of Fe(III) oxyhydroxides

Lepidocrocite, ferrihydrite and goethite were synthesized following established protocols (Boland et al., 2014; Schwertmann and Cornell, 2000; Thies-Weesie et al., 2007). For lepidocrocite synthesis, 11.93 g of $FeCl_2 \cdot 4H_2O$ were dissolved into 300 mL of DI water under stirring conditions. The pH was adjusted to 6.7–6.9 by 1 M NaOH. The solution was oxidized by air which was purged at a rate of 100 mL/min until the pH stabilized and the color turned to orange (Schwertmann and Cornell, 2000). For goethite synthesis, 1 M NaOH solution was added slowly to 250 mL of 0.1 M $Fe(NO_3)_3$ solution under stirring conditions to raise the pH to 11–12 (Thies-Weesie et al., 2007). The resulting solution was aged for 9 days in the dark at room temperature. For ferrihydrite synthesis, 1 M KOH solution was added to 250 mL of 0.1 M $Fe(NO_3)_3$ solution under stirring conditions until pH rose to 7 (Boland et al., 2014). The

suspensions were washed three times with DI water, re-suspended in DI water to make stock solutions, and kept at 4 °C. The main compositions of the synthesized minerals were confirmed by X-ray diffractions (Fig. A1 in Appendix A). Properties of pyrite ($FeS_2$) and mackinawite (FeS) standards have been described in our previous studies (Cheng et al., 2016; Zhang et al., 2016). These standards were used to examine the formation of $FeS_2$ and FeS in the suspensions during characterizations.

### 2.3. Measurement of •OH production in sulfide/Fe(III)/$O_2$ systems

All the batch experiments were conducted in 100-mL reactors which were enwrapped with an aluminium foil to avoid potential photochemical reactions. A fiber-optic oxygen meter (Fibox 4, PreSens GmbH, Regensburg, Germany) with an oxygen probe was glued on the inner side of the reactor for dissolved oxygen (DO) measurement. A certain volume of lepidocrocite stock solution was added to 50 mL of 20 mM BA solution to produce the final concentration of 11.2 mM Fe (or 1 g/L). Note that 20 mM BA could capture over 90% of the •OH which was produced under most experimental conditions (Section A1 in Appendix A). The suspension pH was buffered at 7.0 by 80 mM boric acid. Boric buffer was used because it does not compete with BA for •OH. Sulfide at different dosages (0, 0.5, 2.5, 5.0 and 7.5 mM) was added to start the reaction. For the sake of simplicity, the term of "sulfide" includes both bisulfide and sulfide. Dilute $H_2SO_4$ was added to assist pH adjustment prior to sulfide addition and also during the course of the reaction in case of pH variation. The reactor was stirred with a magnetic stirring bar and covered loosely by an aluminium foil so that the suspensions were exposed to air for oxygenation. Regarding different Fe(III) oxyhydroxides, lepidocrocite was replaced by ferrihydrite or goethite at the same concentration of 11.2 mM Fe, and sulfide dosage was fixed at 0.5 mM. Control experiments without addition of Fe(III) oxyhydroxides or sulfide were performed under the same conditions. Control experiments under anoxic conditions were also carried out with addition of sulfide to lepidocrocite suspensions. At different time intervals, a certain volume of suspension was taken for analysis of cumulative •OH, dissolved S(-II), total and dissolved Fe(II). Because of the volume required for analysis, experiments in parallel were conducted for different sampling events.

To simulate the long-term discharge or leakage of sulfide-containing waters into Fe(III)/$O_2$ environments, •OH production was further measured by multiple additions of low concentrations of sulfide. The same reactor as described above was used, and lepidocrocite suspensions (11.2 mM Fe) were tested. The sulfide dosage was fixed at 5 mM, but this dosage was attained by 5, 10 or 15 sulfide additions. The time interval between two additions was maintained at 30 min according to the results obtained in single addition modes. All the experiments were carried out for 8 h. Suspension samples were taken for analysis at predetermined time intervals. Note that the suspensions were sampled prior to sulfide addition when the time of sampling and addition overlapped. All the above experiments were conducted in duplicate.

### 2.4. Oxidation of phenol by the •OH produced

In lepidocrocite suspensions (11.2 mM Fe) at pH 7, phenol instead of BA was added to produce a final concentration of 1 mg/L (10.6 μM). Then, a total of 10 mM sulfide was added in 20 times (0.5 mM for each addition) with an addition interval of 30 min. To examine the involvement of •OH for phenol oxidation, 100 mM 2-propanol was added because it scavenges •OH efficiently ($k_{2\text{-propanol},\ ^{\bullet}OH} = 1.9 \times 10^9\ M^{-1}\ s^{-1}$ (Buxton et al., 1988)). Control experiments with phenol or lepidocrocite only were carried out under the same conditions. At different time intervals, suspension samples were taken for analysis of dissolved phenol concentration.

### 2.5. Chemical analysis

For the measurement of *p*-HBA that was produced from BA oxidation by •OH, 1 mL of suspension sample was filtered through a 0.22-μm nylon membrane. About 1 mL of methanol was added immediately into the filtrate to quench further oxidation by •OH. *p*-HBA was analyzed by an LC-15C HPLC (Shimadzu) equipped with a UV detector and an Inter Sustain C18 column (4.6 × 250 mm) at the detection wavelength of 255 nm. The mobile phase was a mixture of 0.1% trifluoroacetic acid aqueous solution and acetonitrile (65:35, v/v). Cumulative •OH concentration was estimated from 5.87 times of *p*-HBA concentration (Section 2 in Appendix A). The detection limit of *p*-HBA is 0.1 μM, which corresponds to 0.59 μM •OH (Zhang et al., 2016). Sulfide was measured by the methylene blue method at 665 nm on a UV-vis spectrophotometer (UV-1800 PC, Shanghai Mapada Spectrum Instrument Co., Ltd.) (Environmental Protection Administration of China, 2002). For phenol analysis, the filtrate was mixed with 1 mL of methanol and analyzed by HPLC. The mobile phase was a mixture of acetonitrile and water (45:55, v/v) at 1 mL/min. The detection wavelength was 210 nm.

For the determination of dissolved Fe(II), a special pretreatment procedure was used to minimize Fe(III) reduction by the residual sulfide during acidification. About 2 mL of suspensions were filtered through a 0.22-μm membrane. The filtrate was purged by $N_2$ and mixed with 0.5 mL of 0.5 mM $H_2SO_4$ while maintaining the $N_2$ flux to remove residual sulfide, and then mixed with 0.5 mL of 2 M NaF, 0.2 mL of 1% 1,10-phenanthroline and 0.5 mL of ammonium acetate buffer for $Fe^{2+}$ measurement at 510 nm (Tamura et al., 1974). Fluoride was added to complex Fe(III) and avoid its interference with Fe(II) determination (Tamura et al., 1974). For the determination of total Fe and total Fe(II), the suspensions were digested by 6 M HCl and shaken at 220 rpm under the dark at room temperature for 24 h. To minimize sulfide interference during digestion, 1 mL of suspension was purged by a high flux of $N_2$ with addition of 2.5 mL of 6 M HCl. Then, total Fe(II) in the digested solution was measured after coloration with 1,10-phenanthroline. For total Fe determination, $Fe^{3+}$ was reduced to $Fe^{2+}$ by hydroxylamine hydrochloride prior to the analysis. The potential influence of sulfide on Fe(II) analysis was verified to be negligible under experimental conditions (Section A3 in Appendix A). Regarding the analysis of dissolved Fe(II) in the presence of BPY, 1 mL of suspension was filtered through a 0.22-μm membrane, and the filtrate was analyzed directly for Fe(II) at 522 nm which is the absorption maximum of the Fe(II)-BPY complex.

### 2.6. Characterizations

The pristine Fe(III) oxyhydroxides were washed three times with DI water, separated by centrifugation at 10000 rpm for 5 min and freeze dried for 24 h. Dry particles were characterized by a multipoint BET (Brunauer, Emmett, and Teller) with $N_2$ adsorption at 77 K on a Micromeritics surface area analyzer (ASAP-2020). The specific surface areas were measured to be 106.7, 275.2 and 86.2 $m^2/g$ for lepidocrocite, ferrihydrite, and goethite, respectively. In order to identify Fe and S species produced in lepidocrocite suspensions with sulfide additions, about 50 mL of suspension samples were taken at 10 min for the tests with single addition of 1 and 5 mM sulfide, and at 1 and 4 h for the tests where sulfide was added 10 times. The suspension samples were purged with $N_2$ for 10 min and centrifuged at 10000 rpm in sealed vials. Then the particles were washed several times with deoxygenated DI water, and dried in an anaerobic glove box (COY, USA) filled with 92% $N_2$

and 8% $H_2$. The dried particles were ground in a mortar with pestle in the glove box. Raman spectra were obtained using a confocal laser micro-Raman spectrometer (Thermo DXR Microscope, USA) equipped with diode laser of excitation at 780 nm and a laser power of 5 mW. Data collection, procession and analysis were done using a Thermo Scientific OMNIC software package. XPS analysis was performed on a VG multilab 2000 X-Ray photoelectron Energy Spectrophotometer (Thermo Fischer Scientific, USA) using a monochromatic Al $K_\alpha$ radiation (Power 300 W) and low energy flooding for charge compensation. The spectra were fitted using a least squares procedure using a Gaussian-Lorentzian shape after subtracting a smart baseline using XPSPEAK 4.1 software.

## 3. Results and discussion

### 3.1. •OH production with sulfide addition to Fe(III) oxyhydroxides suspensions

Under neutral and oxic conditions, significant •OH was measured in lepidocrocite, ferrihydrite or goethite suspensions (11.2 mM Fe) with addition of 0.5 mM sulfide (Fig. 1). In the control experiments without sulfide or Fe(III) oxyhydroxides, cumulative •OH was always below the detection limit of 0.59 μM. Addition of sulfide to lepidocrocite under anoxic conditions did not produce any significant level of •OH (Fig. A5). Therefore, $O_2$, sulfide and Fe(III) oxyhydroxides were necessary for •OH production. For 120 min reaction, the cumulative •OH concentration reached 14.2, 14.3 and 22.4 μM for lepidocrocite, ferrihydrite and goethite, respectively. Regarding the time profile, •OH accumulation was fast in the initial 10 min for all the three minerals, stabilized after 10 min for lepidocrocite and ferrihydrite, and increased slowly after 10 min for goethite. This difference can be attributed to the different surface site concentrations and reactivity toward sulfide. The specific surface areas were 106.7, 275.2 and 86.2 $m^2/g$ for lepidocrocite, ferrihydrite, and goethite, respectively (Table 1). Using a site density of $6.3 \times 10^{-6}$ $mol/m^2$ for all the three minerals (Peiffer and Gade, 2007), the surface site concentrations were calculated to be 0.67, 1.80 and 0.54 mM for lepidocrocite, ferrihydrite, and goethite (11.2 mM Fe), respectively (Table 1). For the reaction with 0.5 mM sulfide, the surface site concentrations for lepidocrocite and ferrihydrite would be in excess, but a rough equivalence is expected for goethite. In addition, goethite has a higher crystalline degree than lepidocrocite and ferrhydrite, which can lead to a slower reaction rate with sulfide (Peiffer et al., 2015; Poulton et al., 2004). As a result, lower instantaneous Fe(II) concentrations were produced in a longer reaction time for goethite reduction by sulfide in comparison with lepidocrocite and ferrihydrite (Poulton et al., 2004; Peiffer et al., 2015; Wan et al., 2017), which is beneficial for •OH production during oxygenation. A similar trend was previously observed for •OH production from $H_2O_2$ activation by ferrihydrite and goethite (Kuei-Jyum et al., 2004). Besides, differences of mineral structure and physico-chemical properties may also lead to differences in •OH production (Valentine and Ann Wang, 1998; Huang et al., 2001). The above results confirm that •OH can be produced significantly with addition of sulfide to Fe(III) oxyhydroxides under neutral and oxic conditions.

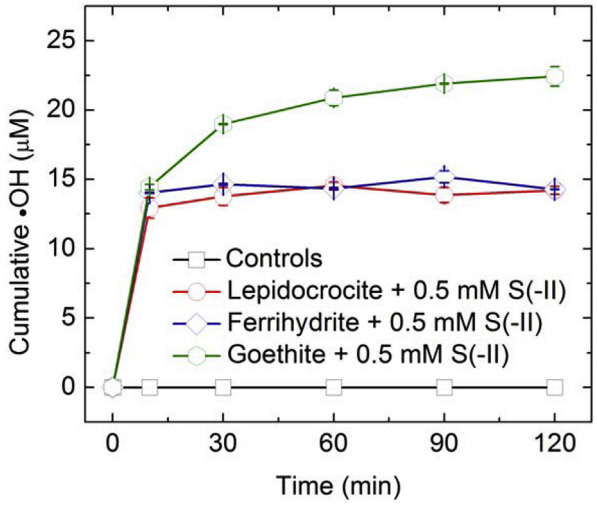


**Fig. 1.** Production of •OH with addition of sulfide to Fe(III) oxyhydroxides suspensions. The reaction conditions were based on 11.2 mM Fe, 20 mM BA, pH 7 and oxic conditions unless otherwise specified. Controls refer to the oxygenation of 0.5 mM S(-II), lepidocrocite, ferrihydrite and goethite individually and also the addition of 2.5 mM sulfide to lepidocrocite suspensions (11.2 mM Fe) under anoxic conditions. Numerical data for plots are provided in Appendix B.

### 3.2. Effect of sulfide dosage on •OH production

Using lepidocrocite as a representative material, •OH production was further explored by varying the dosage of sulfide added. For lepidocrocite suspensions (11.2 mM Fe) under neutral and oxic conditions, the cumulative •OH concentration within 120 min increased from 0 to 14.2, 25.2, 52.6 and 63.1 μM with the increase in sulfide dosage from 0 to 0.5, 2.5, 5 and 7.5 mM, respectively (Fig. 2a). At dosages $\leq$5 mM, •OH accumulation was fast in the initial stage and stabilized afterwards. At dosage of 7.5 mM, •OH accumulation was still operational, although slower, for the reaction time longer than 60 min. The duration of the initial stage for fast •OH accumulation increased with sulfide dosage. As sulfide was the source of electrons for •OH production, a higher sulfide dosage led to a longer time of •OH production in the presence of excess $O_2$. The cumulative •OH concentrations correlated with the dosage of sulfide ($R^2 = 0.980$, Fig. A6 in Appendix A), which further suggests that sulfide drove •OH production.

In parallel to •OH accumulation, sulfide was consumed mostly in the first 10 min and was depleted in the end (Fig. 2b). Control experiments with sulfide only reveal that the loss due to volatilization and/or oxidation by DO was much lower compared to lepidocrocite suspensions (Fig. A7 in Appendix A). This suggests that sulfide reacted with lepidocrocite quickly under the tested conditions. With a surface site concentration of 0.67 mM (Table 1), it is not likely that sulfide at $\geq$ 2.5 mM could be depleted by the pristine surface sites. The quick consumption of sulfide points to the rapid regeneration of surface sites. The total Fe(II) concentration increased quickly after sulfide addition, reached the peak value at the first sampling time of 10 min, and decreased thereafter (Fig. 2c). The peak concentration at 10 min increased from 0 to 3.94 mM with the increase in sulfide dosage from 0 to 7.5 mM (Fig. 2c), showing a good linear dependence on sulfide dosage ($R^2 = 0.995$, Fig. A8 in Appendix A). The variation of dissolved Fe(II) concentration demonstrated a similar trend (Fig. A9 in Appendix A). However, the peak concentrations of dissolved Fe(II) were orders of magnitude

**Table 1**
Characteristics of Fe(III) oxyhydroxides.

| Fe(III) oxyhydroxides | Specific surface area ($m^2/g$) | Surface area concentration ($m^2/L$) | Surface site concentration[a] (mM) |
|---|---|---|---|
| Lepidocrocite | 106.7 | 106.7 | 0.67 |
| Ferrihydrite | 275.2 | 286.6 | 1.80 |
| Goethite | 86.2 | 86.2 | 0.54 |

[a] Surface site concentrations were calculated based on a site density of $6.3 \times 10^{-6}$ $mol/m^2$ for all the three minerals (Peiffer and Gade, 2007).

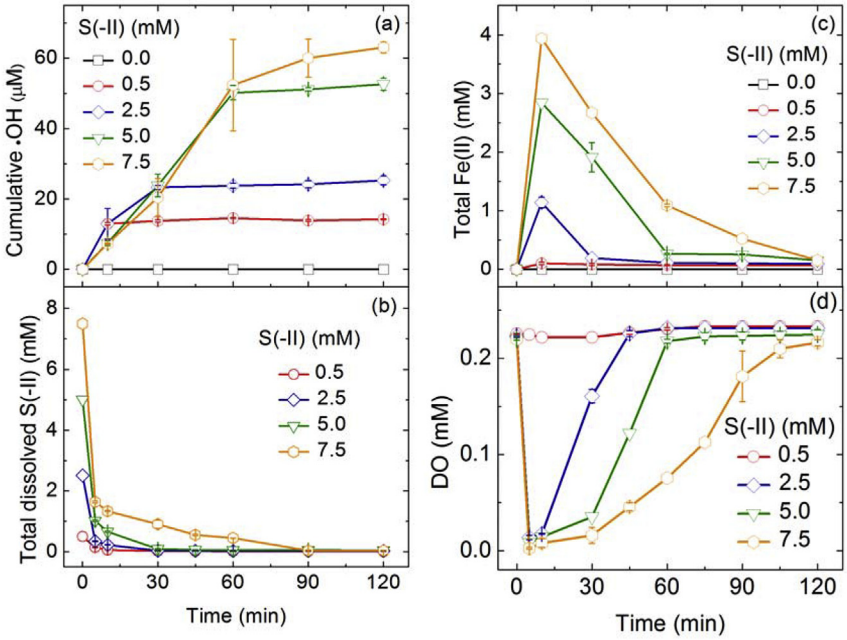


**Fig. 2.** Variations of (a) cumulative •OH concentration, (b) total dissolved sulfide concentration, (c) total Fe(II) concentration, and (d) DO concentration with single addition of sulfide to lepidocrocite suspensions. The reaction conditions were based on 11.2 mM Fe, 20 mM BA, pH 7 and oxic conditions unless otherwise specified. Numerical data for plots are provided in Appendix B.

lower than those of total Fe(II), reflecting the predominance of solid Fe(II) in the suspensions. Accumulation of Fe(II) is determined by the balance between its production from lepidocrocite reduction and its consumption by $O_2$ through oxidation. At a certain DO concentration, a higher sulfide dosage produced more Fe(II) in the initial stage. As measured, the DO concentration dropped drastically from the initial saturation value (0.22 mM) to the lowest value at 5 min after sulfide addition (Fig. 2d), which implies DO was almost totally consumed for Fe(II) oxidation in the initial 5 min. Afterwards, the DO concentration restored gradually to the saturation value, and thus, total Fe(II) decreased gradually.

### 3.3. Enhancement of •OH production by multiple sulfide additions

Production of •OH was further tested by multiple additions of sulfide to lepidocrocite suspensions (11.2 mM Fe) under neutral and oxic conditions. The cumulative sulfide dosage attained in a number of sulfide additions was fixed at 5 mM and the time interval between consecutive additions was 30 min. In all the cases the reaction was monitored for 8 h. The cumulative •OH concentration increased from 52.6 to 101.7, 116.6 and 130.7 μM when the number of additions increased from 1 to 5, 10 and 15, respectively, within 8 h reaction (Fig. 3a). This clearly suggests that the increase of the number of additions boosted •OH production at a fixed dosage of total sulfide. •OH accumulation was fast in the initial stage and stabilized in the later stages when the additions were 10 or less. Nonetheless, •OH accumulation increased always within 8 h in case of 15 additions, which could be ascribed to the relatively longer duration time (7 h) of additions (note that the first addition was carried out at t = 0 h). The prominent increase in •OH accumulation with the number of sulfide additions further supports the hypothesis that sulfide drives •OH production in lepidocrocite/$O_2$ suspensions.

During the course of the reaction, the sulfide that was added in the first time was fully depleted, but the sulfide that was added from the second time onwards could not be fully depleted (Fig. 3b). The residual concentrations of sulfide varied between 0.1 and 0.04 mM from 4 to 8 h. The variation of total Fe(II) was different depending on the number of additions. The total Fe(II) concentration increased in the initial stage and stabilized afterwards for 5 and 10 additions, while it increased continuously for 15 additions (Fig. 3c). The trend of Fe(II) variation was in good agreement with that of •OH accumulation (Fig. 3a and c). For multiple additions, Fe(II) can be produced progressively by lepidocrocite reduction in each addition, but at the same time it can be oxidized by $O_2$. The DO concentration fluctuated during multiple additions, and near saturation was restored at the end of each addition (Fig. A10 in Appendix A). The different patterns of variations of Fe(II) and DO concentrations were mainly attributed to the difference in sampling time for Fe(II) and DO analysis. As the total Fe(II) concentration did not decrease in the later stage when DO concentration was near saturation for 5 and 10 additions, the progressive Fe(II) accumulation can be attributed to other reasons than DO concentration, which will be discussed later.

### 3.4. Effect of BPY on •OH production in single and multiple addition modes

To explore the Fe(II) species contributing to •OH production, BPY was added to complex the dissolved and weakly surface-bound Fe(II), thus screening their contribution (Katsoyiannis et al., 2008). For the tests with single addition of 1 mM sulfide, the presence of 2 mM BPY led to negligible difference in •OH accumulation (Fig. 4a). The Fe(II) complexed by BPY was 0.29 mM (Fig. A11a in Appendix A), which was much higher than the dissolved Fe(II) concentrations measured in the absence of BPY (<4 μM, Fig. A11b in Appendix A). This difference could be ascribed to the complexation of weakly surface-bound Fe(II) by BPY. As the complexation did not significantly affect •OH accumulation, it is reasonable that the dissolved and weakly surface-bound Fe(II) contributed negligibly to •OH production for the single addition of 1 mM sulfide.

For a single addition of 5 mM sulfide, the presence of 2 mM BPY

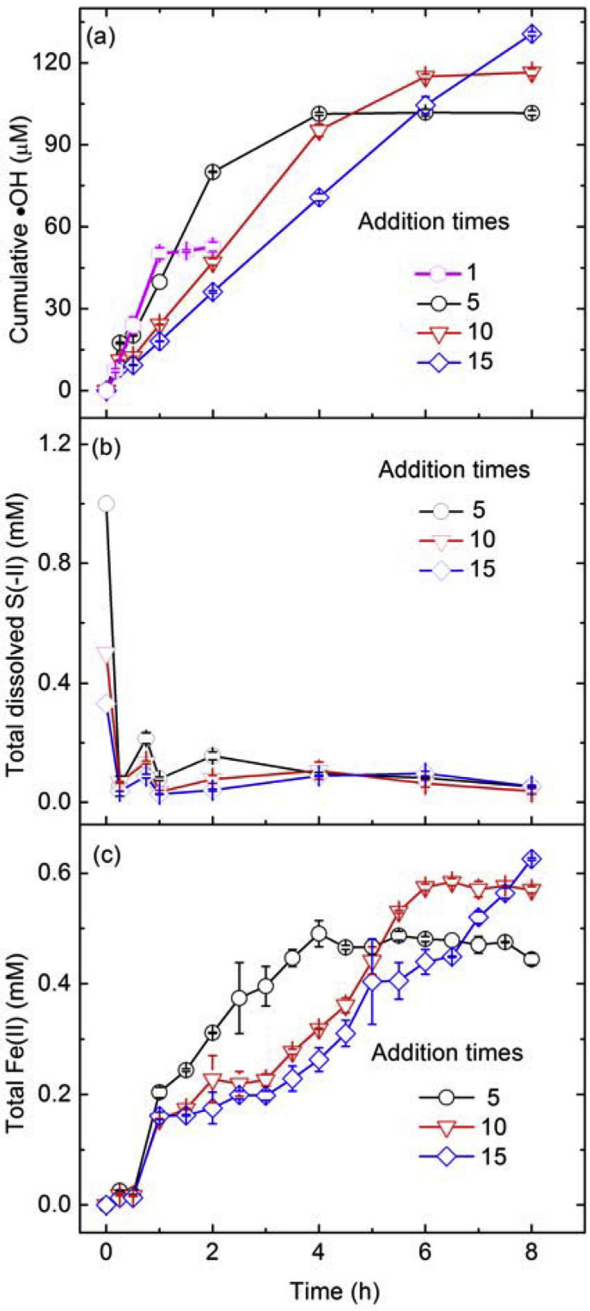


**Fig. 3.** Variations of (a) cumulative •OH concentration, (b) total dissolved sulfide concentration, (c) total Fe(II) concentration with multiple additions of sulfide to lepidocrocite suspensions. The reaction conditions were based on 11.2 mM Fe, 20 mM BA, an addition interval of 30 min, pH 7 and oxic conditions unless otherwise specified. The total concentration of sulfide was fixed at 5 mM, and the dosage added each time equals to 5 mM divided by the number of sulfide additions. The last time of sulfide addition was at 2, 4.5 and 7 h for the additions of 5, 10 and 15, respectively. The sampling was done prior to sulfide addition when the time conflicted. Numerical data for plots are provided in Appendix B.

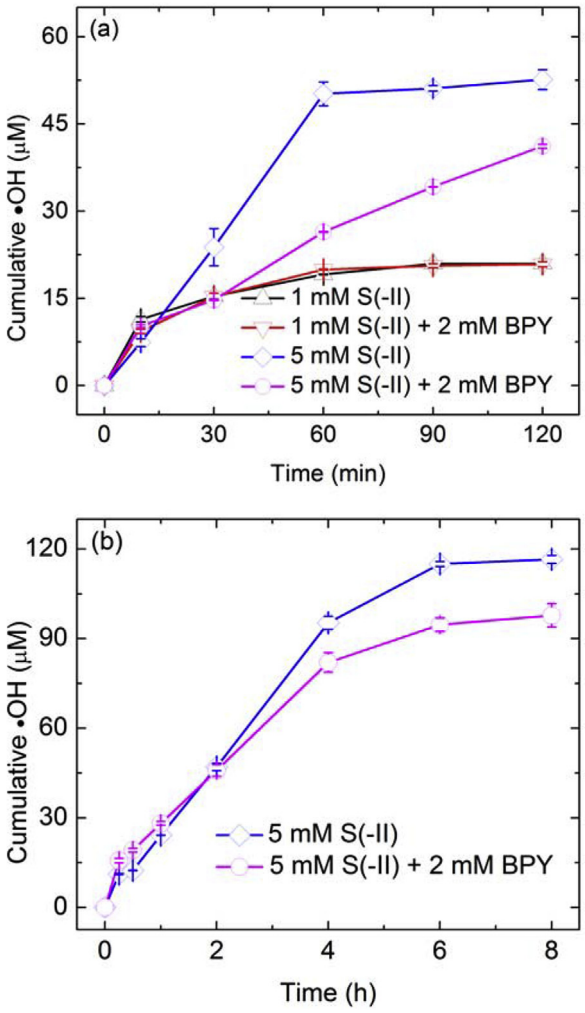


**Fig. 4.** Effect of BPY on •OH accumulation with (a) single and (b) 10 sulfide additions to lepidocrocite suspensions. The reaction conditions were based on 11.2 mM Fe, 20 mM BA, pH 7 and oxic conditions unless otherwise specified. The addition interval was 30 min for multiple additions. Numerical data for plots are provided in Appendix B.

decreased greatly the cumulative •OH concentration (Fig. 4a). The inhibition in •OH accumulation was 52.2% and 21.7% within 60 and 120 min, respectively. In contrast, little inhibition could be observed with single addition of 1 mM sulfide. With single addition of 5 mM sulfide, lepidocrocite reduction produced high Fe(II) concentrations quickly. Consequently, a fraction of free Fe(II) could be complexed by BPY (Fig. A11). It is noteworthy that •OH production ceased after 60 min in the absence of BPY, but the production continued until 120 min in the presence of BPY. This difference could be attributed to the complexation effect caused by BPY. The dissolved and weakly surface-bound Fe(II) can be oxidized quickly by $O_2$ under neutral conditions with formation of Fe(III) precipitates (Keenan and Sedlak, 2008a, 2008b). These precipitates may cover the solid Fe(II) species and inhibit their oxidation. Nonetheless, BPY could complex the dissolved and weakly surface-bound Fe(II) and thus slowed down their oxidation to form Fe(III) precipitates on solid Fe(II) species. So, the reactive solid Fe(II) species could still be oxidized after 60 min.

For the tests with 10 additions, the presence of 2 mM BPY negligibly impacted •OH accumulation for the first 4 additions (initial 2 h), but slightly decreased the cumulative •OH afterwards (Fig. 4b). Similarly, the concentrations of Fe(II) complexed by BPY were much higher than the dissolved Fe(II) concentrations without BPY (Fig. A12 in Appendix A). As the initial concentration of sulfide was low for 10 additions, the influence of BPY in the initial stage was similar to that for a single addition of 1 mM sulfide. In the later stage, the increase of sulfide additions increased Fe(II) production, enhancing the complexation by BPY. However, the maximum inhibition was less than 16.2% after 8 h.

### 3.5. Spectroscopic characterizations of solid particles

For single additions of 1 and 5 mM sulfide, the suspension particles were separated after 10 min of reaction because Fe(II) concentrations peaked at this time. Raman spectra in Fig. 5 show obvious absorption peaks at 87.5, 157, 223, 440 and 477 $cm^{-1}$ for the particles after single addition of 1 mM sulfide. Both the positions and relative intensities were similar to those of elemental sulfur. The peaks for lepidocrocite appeared but at lower intensities compared with the standard. With a single addition of 5 mM sulfide, the peak positions were almost the same as those of a single addition of 1 mM sulfide, but the peak intensities decreased drastically. For 10 min reaction, Fe(II) concentration produced in the test of a single addition of 5 mM sulfide was much higher than that of a single addition of 1 mM sulfide. Virtually, black color (FeS is black) was visibly observed immediately after a single addition of 5 mM sulfide (Fig. A13 in Appendix A). As the FeS standard did not show any significant Raman absorption peaks (Fig. 5), we cannot exclude its appearance. Instead, all the evidence points to the appearance of FeS. For 10 additions of a total of 5 mM sulfide, Fig. 5 shows clear absorption peaks for lepidocrocite at 1 and 4 h but the occurrence of elemental sulfur was obvious only at 4 h. The black color could be only observed for the first addition in the experiments with 5 additions (Fig. A14 in Appendix A). As the addition interval was 30 min for the multiple additions, the particles could be oxidized for at least 30 min after sulfide addition. As a result, elemental sulfur accumulated progressively with time.

For the samples taken after 10 min of single additions of 1 and 5 mM S(-II), Fe($2p_{3/2}$) XPS spectra show that Fe(III) predominated among the surface Fe species, and the occurrence of Fe(II)-S, Fe(III)-S and Fe(II)-O was reflected by the fitted peaks at 707.2, 708.5 and 709.4 eV, respectively (Fig. 6a–b) (Eggleston et al., 1996; Mullet et al., 2002; Thomas et al., 1998). By increasing S(-II) concentration from 1 to 5 mM, the Fe(III) fraction decreased whereas the fractions of the other three species increased (Table A1 in Appendix A). This observation suggests the dependence of surface Fe speciation on S(-II) concentration. S(2p) XPS spectra characterized the presence of sulfide, elemental sulfur and polysulfides (Figs. A15a-b). Similarly, Fe(2p3/2) XPS spectra reveal that Fe(III) predominated among the surface Fe species for the suspension particles after 1 and 4 h reaction with 10 additions of a total of 5 mM sulfide (Fig. 6c–d). However, a small fraction of surface Fe(II) was reflected by the absorption at 709.6 and 709.8 eV for the particles after 1 and 4 h reaction (Descostes et al., 2000; Thomas et al., 1998; Yamashita and Hayes, 2008). The peak area for surface Fe(II) increased slightly when the reaction time increased from 1 to 4 h, which was consistent with the progressive accumulation of Fe(II) upon multiple additions (Fig. 3c). S(2p) XPS spectra suggest the production of elemental sulfur and other sulfur-containing compounds (Figs. A15c-d in Appendix A). In particular, both $S_2^{2-}$ and $S_n^{2-}$ appeared and their relative percentage increased with reaction time, which may suggest the production of pyrite.

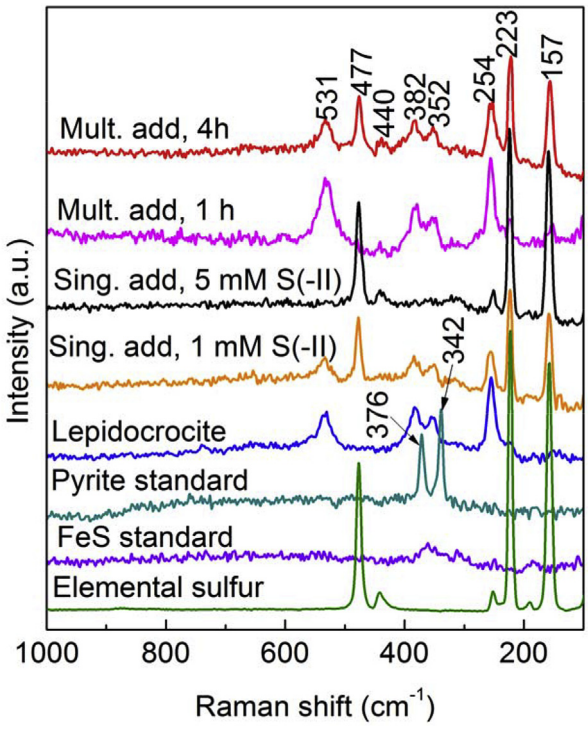


**Fig. 5.** Raman spectra for the suspension particles. The reaction conditions were based on 11.2 mM Fe in lepidocrocite suspensions, 20 mM BA and pH 7 unless otherwise specified. For single addition of 1 and 5 mM S(-II), the samples were taken at 10 min reaction. For multiple additions, samples were taken at 1 and 4 h for the experiments of 10 sulfide additions. To facilitate comparison, the peak intensity for elemental sulfur has been divided by 100.

### 3.6. Proposed mechanisms for •OH production in sulfide/Fe(III)/$O_2$ suspensions

As sulfide or Fe(III) alone cannot produce significant •OH under oxic conditions, and Fe(II) is effective in activating $O_2$ to generate ROS (Liu et al., 2014; Hou et al., 2017), it is reasonable to conclude that sulfide functioned mainly to supply Fe(II) for ROS production through the reduction of Fe(III). From BPY results, dissolved and weakly surface-bound Fe(II) contributed slightly to •OH production. Dissolved Fe(II) concentrations in single addition in the presence of BPY were several orders of magnitude lower than the total Fe(II) concentrations. These results suggest that •OH production could be ascribed mainly to Fe(II) in the solid phase. It has been documented that Fe(II) can sequentially activate $O_2$ to generate $O_2^{\cdot-}$ and $H_2O_2$ through the Haber-Weiss mechanism (King et al., 1995; Rose and Waite, 2002). However, whether Fe(II) can further activate $H_2O_2$ to generate •OH under neutral conditions depends on its speciation. Aqueous $Fe^{2+}$ mainly activate $H_2O_2$ to generate Fe(IV) instead of •OH under neutral conditions (Keenan and Sedlak, 2008a; Hug and Leupin, 2003), whereas Fe(II) complexed by oxygen-containing groups (i.e., organic acids, mineral surface -OH groups) and structural Fe(II) in a range of minerals (i.e., FeS, $FeCO_3$, nontronites) can activate $H_2O_2$ to generate •OH (Cheng et al., 2016; Miller et al., 2016; Tong et al., 2016; Zhu et al., 2017). Therefore in sulfide/Fe(III)/$O_2$ suspensions, •OH production can be presumably attributed to the activation of $O_2$ by the reactive Fe(II) species produced from Fe(III) reduction by sulfide.

To explore the reactive Fe(II) species for •OH production, we referred to the well-established mechanism of Fe(III) oxyhydroxides reduction by sulfide (Dos Santos Afonso and Stumm, 1992; Poulton et al., 2004; Hellige et al., 2012). The reduction of Fe(III) oxyhydroxides by sulfide involves the formation of an inner-sphere surface complex (Eq. (5)), electron transfer from S(-II) to > Fe(III) (Eq. (6)), release of a sulfur radical (Eq. (7)) and detachment of >Fe(II) to the solution (Eq. (8)) (Dos Santos Afonso and Stumm, 1992). The final step of >Fe(II) detachment is the rate limiting step controlled by surface sulfide concentration. In the presence of excess sulfide, the detached $Fe^{2+}$ may transform to FeS (Eq. (9)). The sulfide radical will reduce an additional > $Fe^{III}OH$ and oxidize into elemental sulfur (Eq. (10)).

$$>Fe^{III}OH + HS^- \leftrightarrow >Fe^{III}S^- + H_2O \quad (5)$$

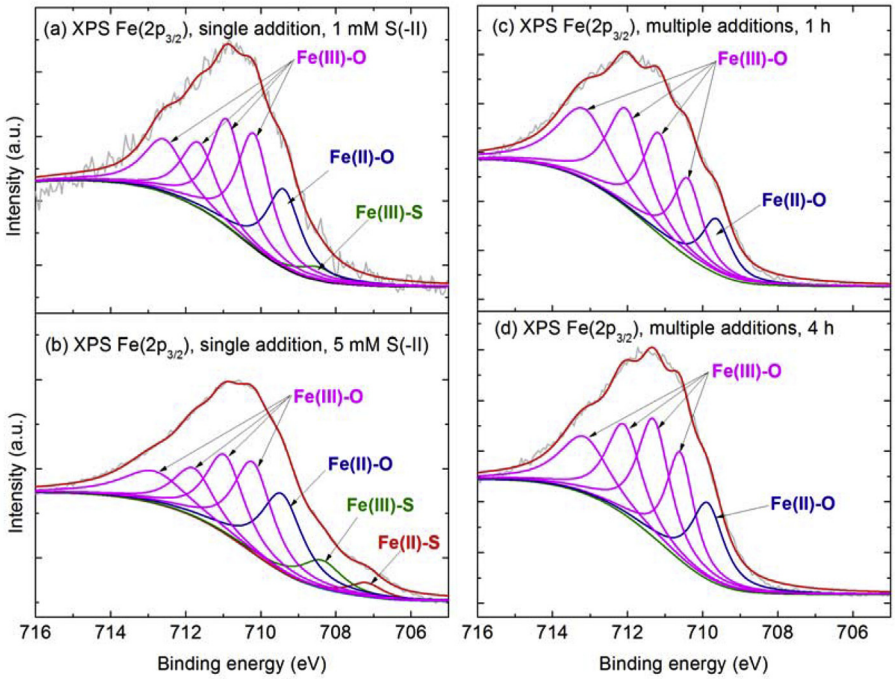


**Fig. 6.** Fe($2p_{3/2}$) XPS spectra for the suspension particles after 10 min reaction for single addition of (a) 1 and (b) 5 mM S(-II), and after (c) 1 and (d) 4 h reaction for 10 sulfide additions. The binding energy and full width at half-maximum of Fe($2p_{3/2}$) for single and multiple additions are shown in Appendix A Table A1 and A2, respectively. The reaction conditions were based on 11.2 mM Fe in lepidocrocite suspensions, 20 mM BA, pH 7 unless otherwise specified.

$$>Fe^{III}S^{-} \leftrightarrow >Fe^{II}S^{\bullet} \quad (6)$$

$$>Fe^{II}S^{\bullet} + H_2O \leftrightarrow >Fe^{II}OH_2^{+} + S^{\bullet-} \quad (7)$$

$$>Fe^{II}OH_2^{+} \rightarrow \text{new reactive site} + Fe^{2+} + H_2O \quad (8)$$

$$Fe^{2+} + HS^{-} \rightarrow FeS + H^{+} \quad (9)$$

$$>Fe^{III}OH + S^{\bullet-} \leftrightarrow > Fe^{2+} + S(0) \quad (10)$$

Accordingly, different Fe(II) species will be produced in sulfide/Fe(III)/$O_2$ suspensions with single and multiple sulfide additions. (a) With single addition of low sulfide dosage (i.e., 0.5 mM), sulfide concentration is lower than the $>Fe^{III}OH$ site concentration (0.67 mM), so sulfide can be oxidized and depleted quickly. Detachment of >Fe(II) from the surface sites in excess is difficult (Hellige et al., 2012). As aqueous $Fe^{2+}$ and sulfide are required for FeS formation (Eq. (9)), and no black solid could be seen in this case, the formation of FeS can be ruled out for single addition of low sulfide dosage. (b) With single addition of high sulfide dosages ($\geq$1 mM), the pristine $>Fe^{III}OH$ site concentration is insufficient, allowing the detachment of >Fe(II) to the solution as $Fe^{2+}$ (Eq. (8)). As a result, FeS could be formed (Eq. (9)). When sulfide is depleted in the initial short time, >Fe(II) may remain in the surface-bound form because of difficult detachment (Hellige et al., 2012; Peiffer et al., 2015; Poulton et al., 2004). As both Fe(II)-S and Fe(II)-O were measured on the surface by XPS, production of FeS and surface-bound Fe(II) in the form of $>Fe^{II}OH_2^{+}$ can be suggested.

In multiple additions mode, sulfide is insufficient relative to $>Fe^{III}OH$ sites in most cases, which does not favor the detachment of $>Fe^{II}OH_2^{+}$ (Eq. (8)) and the subsequent formation of FeS (Eq. (9)) (Hellige et al., 2012; Peiffer et al., 2015). For a certain dosage of sulfide, the increase of the number of sulfide additions results in the decrease in the ratio of sulfide to $>Fe^{III}OH$ site concentration as well as the increase in the cycling between $>Fe^{III}OH$ and $>Fe^{II}OH_2^{+}$. Therefore, surface-bound Fe(II) is the most likely species for •OH production.

In summary, surface-bound Fe(II), most likely in the form of $>Fe^{II}OH_2^{+}$, and FeS are the two Fe(II) species that are most likely to contribute to •OH production in neutral sulfide/Fe(III)/$O_2$ systems. Both surface-bound Fe(II) and FeS have been previously reported to activate $H_2O_2$ and/or $O_2$ for generating •OH under neutral conditions (Cheng et al., 2016; Hou et al., 2017; Yan et al., 2016). The mechanism of •OH production in sulfide/Fe(III)/$O_2$ suspensions can be summarized as generation of reactive Fe(II), in the forms of $>Fe^{II}OH_2^{+}$, and likely FeS, and production of •OH through $O_2$ activation by the reactive Fe(II). •OH production is expected to continue until the depletion of either sulfide or $O_2$. Cycling between Fe(III) reduction and Fe(II) oxidation in different forms is an important feature of the sulfide/Fe(III)/$O_2$ systems for •OH production, which is different from Fe(II)/$O_2$ systems wherein specific Fe(II) species exist.

### 3.7. Phenol oxidation in oxic lepidocrocite suspensions with sulfide additions

In lepidocrocite suspensions (11.2 mM Fe) under neutral and oxic conditions, phenol at 1 mg/L was oxidized progressively by multiple additions of sulfide (Fig. 7). This mode of sulfide addition was adopted because by increasing the number of sulfide additions, the cumulative •OH concentrations increased as well. For 20 additions of a total of 10 mM sulfide (0.5 mM S(-II) per addition), phenol concentration decreased slowly to 0.72 mg/L. Control experiments without sulfide addition showed negligible removal, which excludes significant phenol loss due to adsorption and volatilization. With the addition of 100 mM 2-propanol, an •OH scavenger ($k_{2\text{-propanol, }^{\bullet}OH} = 1.9 \times 10^9\ M^{-1}\ s^{-1}$ (Buxton et al., 1988)), phenol removal was inhibited greatly. Thus, •OH was the predominant reactive species for phenol oxidation. Both sulfide and Fe(II) competed with phenol for •OH. The rate constants for oxidation of

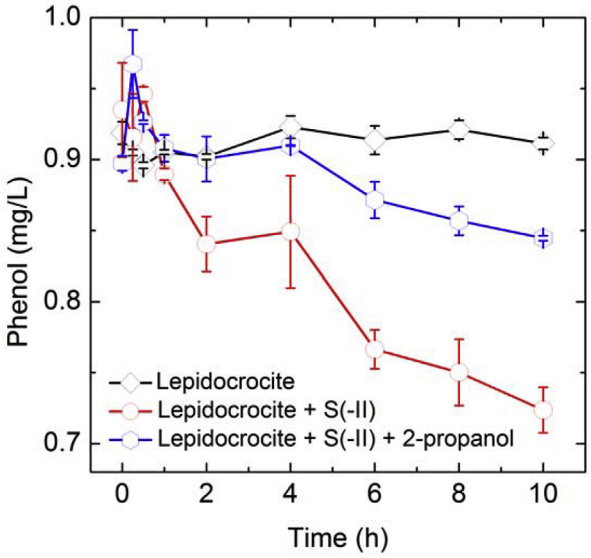


**Fig. 7.** Oxidation of phenol in lepidocrocite suspensions with multiple sulfide additions. The reaction conditions were based on 11.2 mM Fe in lepidocrocite suspensions, 1 mg/L phenol, 20 sulfide additions with 30 min addition interval, pH 7 and oxic conditions unless otherwise specified. The total concentration of sulfide was 10 mM. Numerical data for plots are provided in Appendix B.

phenol and sulfide (in $HS^-$) by •OH are $6.6 \times 10^9$ and $9.0 \times 10^9\ M^{-1}\ s^{-1}$, respectively (Buxton et al., 1988). The rate constant for oxidation of >Fe(II) by •OH is unknown, but it can be assumed to be lower than that of aqueous $Fe^{2+}$ ($3.2 \times 10^8\ M^{-1}\ s^{-1}$ (Buxton et al., 1988)) because of the mass transfer resistance in heterogeneous systems. As the rate constants for phenol and sulfide are close and at least one order of magnitude higher than that for > Fe(II), an effective utilization of •OH for phenol oxidation necessitates a higher concentration of phenol than sulfide. At the initial phenol concentration of 1 mg/L (= 10.6 μM), an effective oxidation of phenol requires that the coexisting sulfide concentration be lower than 10.6 μM. This implies that most of phenol oxidation occurred only when the added sulfide was consumed to a concentration lower than 10.6 μM. Thus, a long-term discharge of low concentrations of sulfide to Fe(III)/$O_2$ systems is presumed to be beneficial to the oxidative transformation of phenol. In multiple sulfide additions, low concentrations of sulfide were added into Fe(III)/$O_2$ systems, leading to a weak competition of sulfide and Fe(II) for •OH and a significant oxidation of phenol. As many contaminants in the environment can be oxidized by •OH at rate constants close to phenol (Buxton et al., 1988; Wojnárovits et al., 2018), the conditions found for phenol oxidation could be also applicable to their oxidation.

## 4. Conclusions

This study investigated the production of •OH upon sulfide addition to Fe(III) oxyhydroxides suspensions under neutral and oxic conditions. •OH was produced with addition of sulfide to different Fe(III) oxyhydroxides, and its cumulative concentration increased with increasing sulfide dosage. For a certain total amount of added sulfide, •OH production was enhanced by increasing the number of sulfide additions. The reduction of Fe(III) by sulfide produced surface-bound Fe(II) and FeS at low and high sulfide concentrations, respectively. As suggested by BPY experiments, Fe(II) in the solid phase or FeS could be produced in addition to surface-bound Fe(II) species. These Fe(II) species were mainly responsible for •OH production. Weakly surface-bound and dissolved Fe(II) species were produced in both addition modes but played a slight role in the production of •OH. The produced •OH could contribute to the oxidative transformation of contaminants under certain conditions. Since the surface-bound Fe(II) identified in this study are highly reactive (Hellige et al., 2012; Li et al., 2019), they might enhance the abiotic degradation of contaminants at Fe(III) oxyhydroxide surfaces (Pecher et al., 2002; Elsner et al., 2004) under oxic conditions. Thus, a cyclic upwelling or diffusion of low sulfide concentrations to oxic Fe(III) systems should enhance •OH production and contaminant degradation. In oxic marine and brackish environments, FeS may form predominantly due to the occurrence of high sulfide and low Fe(III) concentrations (van der Welle et al., 2006) and could determine the fate of the contaminants in these environments. Our findings add a new pathway, sulfide perturbation of Fe(III)/$O_2$ systems, to the scenario of •OH production in natural environments.

## Acknowledgments

This work was supported by the Natural Science Foundation of China (No. 41830862, 41772374, 41521001), Natural Science Foundation of Hubei Province, China (2018CFA028) and the 111 Program of State Administration of Foreign Experts Affairs & the Ministry of Education of China (B18049).

## Appendix A. Supplementary data

Supplementary data to this article can be found online at https://doi.org/10.1016/j.chemosphere.2019.06.037.

## References

Boland, D.D., Collins, R.N., Miller, C.J., et al., 2014. Effect of solution and solid-phase conditions on the Fe(II)-accelerated transformation of ferrihydrite to lepidocrocite and goethite. Environ. Sci. Technol. 48, 5477–5485. https://doi.org/10.1021/es4043275.

Brüchert, V., Jørgensen, B.B., Neumann, K., Riechmann, D., Schlösser, M., Schulz, H., 2003. Regulation of bacterial sulfate reduction and hydrogen sulfide fluxes in the central namibian coastal upwelling zone. Geochem. Cosmochim. Acta 67, 4505–4518. https://doi.org/10.1016/S0016-7037(03)00275-8.

Buxton, G.V., Greenstock, C.L., Helman, W.P., et al., 1988. Critical review of rate constants for reactions of hydrated electrons, hydrogen atoms and hydroxyl radicals (•OH/•$O^-$) in aqueous solution. J. Phys. Chem. Ref. Data 17, 513–886. https://doi.org/10.1063/1.555805.

Cheng, D., Yuan, S., Liao, P., et al., 2016. Oxidizing Impact Induced by Mackinawite (FeS) Nanoparticles at oxic conditions due to production of hydroxyl radicals. Environ. Sci. Technol. 50, 11646–11653. https://doi.org/10.1021/acs.est.6b02833.

Descostes, M., Mercier, F., Thromat, N., et al., 2000. Use of XPS in the determination of chemical environment and oxidation state of iron and sulfur samples: Constitution of a data basis in binding energies for Fe and S reference compounds and applications to the evidence of surface species of an oxidized pyrite in carbonate medium. Appl. Surf. Sci. 165, 288–302. https://doi.org/10.1016/S0169-4332(00)00443-8.

Dos Santos Afonso, M., Stumm, W., 1992. Reductive dissolution of iron(III) (hydr) oxides by hydrogen sulfide. Langmuir 8, 1671–1675 https://doi.org/10.1021/la00042a030.

Eggleston, C.M., Ehrhardt, J.J., Stumm, W., 1996. Surface structural controls on pyrite oxidation kinetics: An XPS-UPS, STM, and modeling study. Am. Mineral. 81, 1036–1056. https://doi.org/10.2138/am-1996-9-1002.

Eggleton, J., Thomas, K.V., 2004. A review of factors affecting the release and bioavailability of contaminants during sediment disturbance events. Environ. Int. 30, 973–980. https://doi.org/10.1016/j.envint.2004.03.001.

Elsner, M., Schwarzenbach, R.P., Haderlein, S.B., 2004. Reactivity of Fe(II)-bearing minerals toward reductive transformation of organic contaminants. Environ. Sci. Technol. 38, 799–807. https://doi.org/10.1021/es0345569.

Environmental Protection Administration of China, 2002. Water and Wastewater Monitoring and Analysis Methods, fourth ed. China Environmental Science Press.

Fazlzadeh, M., Rostami, R., Norouzian Baghani, A., Hazrati, S., Mokammel, A., 2018. Hydrogen sulfide concentrations in indoor air of thermal springs. Hum. Ecol. Risk Assess. 24, 1441–1452. https://doi.org/10.1080/10807039.2017.1413537.

Fenchel, T., 1969. The ecology of marine microbenthos IV. Structure and function of the benthic ecosystem, its chemical and physical factors and the microfauna commuities with special reference to the ciliated protozoa. Ophelia 6, 1–182. https://doi.org/10.1080/00785326.1969.10409647.

Giampaoli, S., Valeriani, F., Gianfranceschi, G., et al., 2013. Hydrogen sulfide in thermal spring waters and its action on bacteria of human origin. Microchem. J. 108, 210–214. https://doi.org/10.1016/j.microc.2012.10.022.
Gómez-Toribio, V., García-Martín, A.B., Martínez, M.J., et al., 2009. Induction of extracellular hydroxyl radical production by white-rot fungi through quinone redox cycling. Appl. Environ. Microbiol. 75, 3944–3953 https://doi.org/10.1128/AEM.02137-08.
Held, I., Wolf, L., Eiswirth, M., et al., 2006. Impacts of sewer leakage on urban groundwater. In: Urban Groundwater Management and Sustainability. Springer, Dordrecht, pp. 189–204.
Hellige, K., Pollok, K., Larese-Casanova, P., et al., 2012. Pathways of ferrous iron mineral formation upon sulfidation of lepidocrocite surfaces. Geochem. Cosmochim. Acta 81, 69–81. https://doi.org/10.1016/j.gca.2011.12.014.
Hou, X., Huang, X., Jia, F., et al., 2017. Hydroxylamine promoted goethite surface Fenton degradation of organic pollutants. Environ. Sci. Technol. 51, 5118–5126. https://doi.org/10.1021/acs.est.6b05906.
Huang, H.-H., Lu, M.-C., Chen, N.J., 2001. Catalytic decomposition of hydrogen peroxide and 2-chlorophenol with iron oxides. Water Res. 35, 2291–2299. https://doi.org/10.1016/S0043-1354(00)00496-6.
Hug, S.J., Leupin, O., 2003. Iron-catalyzed oxidation of arsenic(III) by oxygen and by hydrogen peroxide: pH-Dependent formation of oxidants in the Fenton reaction. Environ. Sci. Technol. 37, 2734–2742. https://doi.org/10.1021/es026208x.
Jayalath, N., Mosley, L.M., Fitzpatrick, R.W., et al., 2016. Addition of organic matter influences pH changes in reduced and oxidised acid sulfate soils. Geoderma 262, 125–132. https://doi.org/10.1016/j.geoderma.2015.08.012.
Katsoyiannis, I.A., Ruettimann, T., Hug, S.J., 2008. pH Dependence of Fenton reagent generation and As(III) oxidation and removal by corrosion of zero valent iron in aerated water. Environ. Sci. Technol. 42, 7424–7430. https://doi.org/10.1021/es800649p.
Keenan, C.R., Sedlak, D.L., 2008a. Factors affecting the yield of oxidants from the reaction of nanoparticulate zero-valent iron and oxygen. Environ. Sci. Technol. 42, 1262–1267. https://doi.org/10.1021/es7025664.
Keenan, C.R., Sedlak, D.L., 2008b. Ligand-enhanced reactive oxidant generation by nanoparticulate zero-valent iron and oxygen. Environ. Sci. Technol. 42, 6936–6941. https://doi.org/10.1021/es801438f.
King, W., Lounsbury, H.A., Millero, F., 1995. Rates and mechanism of Fe(II) oxidation at nanomolar total iron concentrations. Environ. Sci. Technol. 29, 818–824. https://doi.org/10.1021/es00003a033.
Kuei-Jyum, Y.C., Wei-Shun, C., Wei-Yi, C., 2004. Production of hydroxyl radicals from the decomposition of hydrogen peroxide catalyzed by various iron oxides at pH 7. Pract. Period. Hazard. Toxic, Radioact. Waste Manag. 8, 161–165. https://doi.org/10.1061/(ASCE)1090-025X(2004)8:3(161).
Li, X., Liu, L., Wu, Y., Liu, T., 2019. Determination of the redox potentials of solution and solid surface of Fe(II) associated with iron oxyhydroxides. ACS Earth Space Chem. 3, 711–717. https://doi.org/10.1021/acsearthspacechem.9b00001.
Lin, K., Song, L., Zhou, S., Chen, D., Gan, J., 2016. Formation of brominated phenolic contaminants from natural manganese oxides-catalyzed oxidation of phenol in the presence of Br–. Chemosphere 155, 266–273. https://doi.org/10.1016/j.chemosphere.2016.04.064.
Liu, W., Ai, Z., Cao, M., et al., 2014. Ferrous ions promoted aerobic simazine degradation with Fe@$Fe_2O_3$ core–shell nanowires. Appl. Catal. B Environ. 150–151, 1–11. https://doi.org/10.1016/j.apcatb.2013.11.034.
Lu, Z., Smyth, S.A., De Silva, A.O., 2019. Distribution and fate of synthetic phenolic antioxidants in various wastewater treatment processes in Canada. Chemosphere 219, 826–835 https://doi.org/j.chemosphere.2018.12.068.
Luther, G., Ma, S., Trouwborst, R., Glazer, B., Blickley, M., Scarborough, R., Mensinger M, G., 2004. The roles of anoxia, $H_2S$, and storm events in fish kills of dead-end canals of Delaware Inland Bays. Estuaries 27, 551–560 https://doi.org/10.1007/BF02803546.
Manning, M.R., Lowe, D.C., Moss, R.C., et al., 2005. Short-term variations in the oxidizing power of the atmosphere. Nature 436, 1001–1004. https://doi.org/10.1038/nature03900.
Miller, C.J., Rose, A.L., Waite, T.D., 2016. Importance of iron complexation for Fenton-mediated hydroxyl radical production at circumneutral pH. Front. Mar. Sci. 3, 1–13. https://doi.org/10.3389/fmars.2016.00134.
Minella, M., De Laurentiis, E., Maurino, V., et al., 2015. Dark production of hydroxyl radicals by aeration of anoxic lake water. Sci. Total Environ. 527–528, 322–327. https://doi.org/10.1016/j.scitotenv.2015.04.123.
Mopper, K., Zhou, X., 1990. Hydroxyl radical photoproduction in the sea and its potential impact on marine processes. Science 250, 661–664. https://doi.org/10.1126/science.250.4981.661.
Moyo, C.E., Beckett, R.P., Trifonova, T.V., et al., 2017. Extracellular redox cycling and hydroxyl radical production occurs widely in lichenized ascomycetes. Fungal Biol. 121, 582–588. https://doi.org/10.1016/j.funbio.2017.03.005.
Mullet, M., Boursiquot, S., Abdelmoula, M., et al., 2002. Surface chemistry and structural properties of mackinawite prepared by reaction of sulfide ions with metallic iron. Geochem. Cosmochim. Acta 66, 829–836. https://doi.org/10.1016/S0016-7037(01)00805-5.
Murphy, S.A., Meng, S., Solomon, B.M., et al., 2016. Hydrous ferric oxides in sediment catalyze formation of reactive oxygen species during sulfide oxidation. Front. Mar. Sci. 3, 1–12. https://doi.org/10.3389/fmars.2016.00227.
Murphy, S.A., Solomon, B.M., Meng, S., et al., 2014. Geochemical production of reactive oxygen species from biogeochemically reduced Fe. Environ. Sci. Technol. 48, 3815–3821. https://doi.org/10.1021/es4051764.
Ohde, T., Dadou, I., 2018. Seasonal and annual variability of coastal sulphur plumes in the northern Benguela upwelling system. PLoS One 13, e0192140. https://doi.org/10.1371/journal.pone.0192140.
Page, S.E., Sander, M., Arnold, W.A., et al., 2012. Hydroxyl radical formation upon oxidation of reduced humic acids by oxygen in the dark. Environ. Sci. Technol. 46, 1590–1597 https://doi.org/doi.org/10.1021/es203836f.
Page, S.E., Kling, G., Sander, M., et al., 2013. Dark formation of hydroxyl radical in arctic soil and surface waters. Environ. Sci. Technol. 47, 12860–12867 https://doi.org/doi.org/10.1021/es4033265.
Payne, M.K., Stolt, M.H., 2017. Understanding sulfide distribution in subaqueous soil systems in southern New England, USA. Geoderma 308, 207–214. https://doi.org/10.1016/j.geoderma.2017.08.015.
Pecher, K., Haderlein, S.B., Schwarzenbach, R.P., 2002. Reduction of polyhalogenated methanes by surface-bound Fe(II) in aqueous suspensions of iron oxides. Environ. Sci. Technol. 36, 1734–1741. https://doi.org/10.1021/es011191o.
Peiffer, S., Behrends, T., Hellige, K., et al., 2015. Pyrite formation and mineral transformation pathways upon sulfidation of ferric hydroxides depend on mineral type and sulfide concentration. Chem. Geol. 400, 44–55. https://doi.org/10.1016/j.chemgeo.2015.01.023.
Peiffer, S., Gade, W., 2007. Reactivity of ferric oxides toward $H_2S$ at low pH. Environ. Sci. Technol. 41, 3159–3164. https://doi.org/10.1021/es062228d.
Pera-Titus, M., Garcıa-Molina, V., Baños, M.A., Giménez, J., Esplugas, S., 2004. Degradation of chlorophenols by means of advanced oxidation processes: A general review. Appl. Catal. B Environ. 47, 219–256. https://doi.org/10.1016/j.apcatb.2003.09.010.
Poulton, S.W., Krom, M.D., Raiswell, R., 2004. A revised scheme for the reactivity of iron (oxyhydr)oxide minerals towards dissolved sulfide. Geochem. Cosmochim. Acta 68, 3703–3715. https://doi.org/10.1016/j.gca.2004.03.012.
Poulton, S.W., Raiswell, R., 2002. The low-temperature geochemical cycle of iron: From continental fluxes to marine sediment deposition. Am. J. Sci. 302, 774–805. https://doi.org/10.2475/ajs.302.9.774.
Reverberi, A., Klemeš, J.J., Varbanov, P.S., et al., 2016. A review on hydrogen production from hydrogen sulphide by chemical and photochemical methods. J. Clean. Prod. 136, 72–80. https://doi.org/10.1016/j.jclepro.2016.04.139.
Reynolds, J.H., Barrett, H., 2003. A review of the effects of sewer leakage on groundwater quality. J. Chart. Inst. Water E. 17, 34–39. https://doi.org/10.1111/j.1747-6593.2003.tb00428.x.
Rose, A.L., Waite, T.D., 2002. Kinetic model for Fe(II) oxidation in seawater in the absence and presence of natural organic matter. Environ. Sci. Technol. 36, 433–444. https://doi.org/10.1021/es0109242.
Schwertmann, U., Cornell, R.M., 2000. Iron Oxides in the Laboratory Preparation and Characterization, second ed. Wiley-VCH.
Tamura, H., Goto, K., Yotsuyanagi, T., et al., 1974. Spectrophotometric determination of iron (II) with 1, 10-phenanthroline in the presence of large amounts of iron (III). Talanta 21, 314–318. https://doi.org/10.1016/0039-9140(74)80012-3.
Thies-Weesie, D.M.E., Hoog, J.P.D., Mendiola, M.H.H., et al., 2007. Synthesis of goethite as a model colloid for mineral liquid crystals. Chem. Mater. 19, 5538–5546. https://doi.org/10.1021/cm071229h.
Thomas, J.E., Jones, C.F., Skinner, W.M., et al., 1998. The role of surface sulfur species in the inhibition of pyrrhotite dissolution in acid conditions. Geochem. Cosmochim. Acta 62, 1555–1565. https://doi.org/10.1016/S0016-7037(98)00087-8.
Tong, M., Yuan, S., Ma, S., et al., 2016. Production of abundant hydroxyl radicals from oxygenation of subsurface sediments. Environ. Sci. Technol. 50, 214–221. https://doi.org/10.1021/acs.est.5b04323.
Tostevin, R., Craw, D., Van Hale, R., et al., 2016. Sources of environmental sulfur in the groundwater system, southern New Zealand. Appl. Geochem. 70, 1–16. https://doi.org/10.1016/j.apgeochem.2016.05.005.
Trusiak, A., Treibergs, L.A., Kling, G.W., et al., 2018. The role of iron and reactive oxygen species in the production of $CO_2$ in arctic soil waters. Geochem. Cosmochim. Acta 224, 80–95. https://doi.org/10.1016/j.gca.2017.12.022.
Valentine, L.R., Ann Wang, H.C., 1998. Iron oxide surface catalyzed oxidation of quinoline by hydrogen peroxide. J. Environ. Eng. 124, 31–38. https://doi.org/10.1061/(ASCE)0733-9372(1998)124:1(31).
van der Welle, M.E.W., Cuppens, M., Lamers, L.P.M., Roelofs, J.G.M., 2006. Detoxifying toxicants: Interactions between sulfide and iron toxicity in freshwater wetlands. Environ. Toxicol. Chem. 25, 1592–1597 https://doi.org/10.1897/05-283R.1.
Vione, D., Falletti, G., Maurino, V., et al., 2006. Sources and sinks of hydroxyl radicals upon irradiation of natural water samples. Environ. Sci. Technol. 40, 3775–3781. https://doi.org/10.1021/es052206b.
Wan, M., Schröder, C., Peiffer, S., 2017. Fe(III): S(-II) concentration ratio controls the pathway and the kinetics of pyrite formation during sulfidation of ferric hydroxides. Geochem. Cosmochim. Acta 217, 334–348. https://doi.org/10.1016/j.gca.2017.08.036.
Wang, W., Kannan, K., 2018. Inventory, loading and discharge of synthetic phenolic antioxidants and their metabolites in wastewater treatment plants. Water Res. 129, 413–418. https://doi.org/10.1016/j.watres.2017.11.028 0043-1354.
Wojnárovits, L., Tóth, T., Takács, E., 2018. Critical evaluation of rate coefficients for hydroxyl radical reactions with antibiotics: A review. Crit. Rev. Environ. Sci. Technol. 0, 1–37. https://doi.org/10.1080/10643389.2018.1463066.
Yamashita, T., Hayes, P., 2008. Analysis of XPS spectra of $Fe^{2+}$ and $Fe^{3+}$ ions in oxide materials. Appl. Surf. Sci. 254, 2441–2449. https://doi.org/10.1016/j.apsusc.2007.09.063.
Yan, W., Zhang, J., Jing, C., 2016. Enrofloxacin transformation on Shewanella oneidensis MR-1 reduced goethite during anaerobic–aerobic transition. Environ. Sci. Technol. 50, 11034–11040. https://doi.org/10.1021/acs.est.6b03054.

Yuan, X., Nico, P.S., Huang, X., et al., 2017. Production of hydrogen peroxide in groundwater at Rifle, Colorado. Environ. Sci. Technol. 51, 7881–7891. https://doi.org/10.1021/acs.est.6b04803.

Zhang, P., Yuan, S., 2017. Production of hydroxyl radicals from abiotic oxidation of pyrite by oxygen under circumneutral conditions in the presence of low-molecular-weight organic acids. Geochem. Cosmochim. Acta 218, 153–166. https://doi.org/10.1016/j.gca.2017.08.032.

Zhang, P., Yuan, S., Liao, P., 2016. Mechanisms of hydroxyl radical production from abiotic oxidation of pyrite under acidic conditions. Geochem. Cosmochim. Acta 172, 444–457. https://doi.org/10.1016/j.gca.2015.10.015.

Zhu, J., Zhang, P., Yuan, S., et al., 2017. Production of hydroxyl radicals from oxygenation of simulated AMD due to $CaCO_3$-induced pH increase. Water Res. 111, 118–126. https://doi.org/10.1016/j.watres.2016.12.048.